

Original Research Article



DDX5 regulates asymmetric division of mouse oocytes by modulating the stability of microfilament-associated protein radixin

Lina Yu ^{a,b,1}, Ruixin Shi ^{c,1}, Yan Mao ^{b,1}, Aolei Guo ^a, Lihua Zhu ^{b,c,*},
Guangyi Cao ^{a,b,**}

^a State Key Laboratory of Reproductive Medicine and Offspring Health, Center for Reproductive Medicine and Obstetrics and Gynecology, Nanjing Drum Tower Hospital Clinical College of Nanjing Medical University, Nanjing, 210008, China

^b Center for Reproductive Medicine and Obstetrics and Gynecology, Nanjing Drum Tower Hospital, Affiliated Hospital of Medical School, Nanjing University, Nanjing, 210008, China

^c Center for Reproductive Medicine and Obstetrics and Gynecology, Joint Institute of Nanjing Drum Tower Hospital for Life and Health, College of Life Science, Nanjing Normal University, Nanjing, 210008, China

ARTICLE INFO

Keywords:

Oocyte
Meiosis
Cytoskeleton
DDX5
Cytokinesis

ABSTRACT

Mammalian oocytes arrest at prophase I and resume meiosis upon germinal vesicle breakdown, leading to asymmetric division and formation of a smaller polar body and larger oocyte, crucial for genome segregation and cytoplasmic distribution. Actin filaments regulate this division, with reorganization involving actin cap formation and cytoplasmic network changes, mediated by actin-binding proteins like myosins and radixin. DDX5, an RNA helicase, is implicated in transcription, RNA metabolism, and early embryonic development, though its regulatory mechanisms in oocyte maturation remain unclear. Here, we demonstrate that DDX5 regulates cytokinesis during mouse oocyte meiotic maturation. DDX5 colocalizes with the spindle upon meiotic resumption, and its inhibition impairs polar body extrusion and cytokinesis. RNA-seq reveals disrupted mRNA homeostasis upon DDX5 depletion, while IP-MS identifies its interaction with actin cytoskeletal proteins, including radixin, whose expression is significantly reduced. Our findings reveal that DDX5 modulates oocyte cytokinesis by regulating actin cytoskeleton dynamics, underscoring its critical role in asymmetric division.

1. Introduction

Mammalian oocytes undergo meiotic maturation prior to fertilization. The oocytes are arrested at the diplotene stage of the first meiotic prophase. Upon germinal vesicle breakdown, the oocytes resume meiosis, followed by microtubule assembly and chromatin segregation. The oocytes then complete the first meiotic division and become arrested at the metaphase stage of the second meiotic division, awaiting fertilization [1,2]. Mammalian oocytes are unique in their ability to undergo asymmetric cell division. Through asymmetric division, oocytes produce a smaller first polar body and a larger oocyte. This asymmetric division plays a crucial role in the correct segregation of the oocyte genome and the highly asymmetric distribution of cytoplasm. The larger oocyte is essential for storing maternal materials and supporting fertilization [3].

Actin filaments are key factors controlling asymmetric division in mouse oocytes. During oocyte maturation, two characteristic events occur in the reorganization of the actin cytoskeleton: the formation of an actin cap in the cortical region near the spindle and dynamic changes in the density of the cytoplasmic actin network [4–6]. The actin cytoskeleton is primarily composed of various actin-binding proteins. Myosins, which are actin-dependent motor proteins, have diverse functions, including the regulation of cytokinesis, cell motility, and cell polarity [5]. The microfilament skeleton also includes structural proteins such as radixin, which can form complexes with ezrin and moesin. These proteins are cytoskeletal components that may be important in linking actin to the plasma membrane [7,8]. Although some progress has been made in understanding the regulation of asymmetric division by the actin cytoskeleton, the mechanisms by which these microfilament proteins are regulated remain unclear.

* Corresponding author. 321 Zhongshan Road, Gulou District, Nanjing City, Jiangsu Province, 210008, China.

** Corresponding author. 321 Zhongshan Road, Gulou District, Nanjing City, Jiangsu Province, 210008, China.

E-mail addresses: juliazhu@163.com (L. Zhu), caogy@njgyl.com (G. Cao).

¹ These authors contributed equally to this work.

DDX5 (DEAD-Box Helicase 5), also known as p68, is a protein belonging to the DEAD-box RNA helicase family. It functions as an ATP-dependent RNA helicase and plays critical roles in various biological processes, including transcriptional regulation, RNA splicing, and miRNA processing [9,10]. Recent studies have shown that DDX5 has important functions in the reproductive system. In the male mouse reproductive system, DDX5 is involved in spermatogenesis, acting as a transcriptional coactivator and interacting with the core reproductive transcription factor PLZF to regulate the expression of key genes and RNA metabolism, ensuring normal sperm development and function [11]. In zebrafish models, a deficiency in DDX5 results in mutants with small ovaries and female infertility [12]. Inhibition of DDX5 activity during the zygotic stage in mouse embryos leads to increased levels of γ -H2AX in both maternal and paternal pronuclei, affecting early embryonic genome activation [13]. Although these studies highlight the important roles of DDX5 in the reproductive system, and proteomic analyses reveal abundant expression of DDX5 in mouse and human oocytes [14], the specific function of DDX5 in mouse oocyte maturation remains unclear.

In this study, we demonstrate that DDX5 regulates cytokinesis during meiotic maturation in mouse oocytes. When oocytes resume meiosis, DDX5 protein exhibits partial colocalization with the spindle. Inhibition of DDX5 function results in a decreased rate of first polar body extrusion and abnormal cytokinesis in oocytes. RNA-seq experiments reveal that loss of DDX5 disrupts mRNA homeostasis in oocytes. IP-MS (Immunoprecipitation-Mass Spectrometry) experiments further demonstrate that DDX5 regulates cytokinesis by influencing the expression of microfilament-associated protein radixin. Our findings reveal that the RNA helicase DDX5 regulates oocyte cytokinesis by modulating the stability of microfilament-associated proteins radixin.

2. Materials and methods

2.1. Animal experiments

The animal experiments in this study were approved by the Institutional Animal Care and Use Committee of Nanjing Drum Tower Hospital (Approval No. SYXK 2019-0059). Three-week-old female ICR mice were obtained from the Animal Center of Nanjing Medical University and housed at the Animal Center of Nanjing Drum Tower Hospital under a 12-h light/dark cycle.

2.2. Oocyte collection and culture

Fully grown oocytes at the germinal vesicle (GV) stage were collected from the ovaries of three-week-old female mice. Superovulation was induced via intraperitoneal injection of 5 IU pregnant mare serum gonadotropin (PMSG). Cumulus-oocyte complexes (COCs) were collected, and cumulus cells were removed through repeated mouth pipetting. Oocytes were then cultured in MEM- α medium supplemented with 3 mg/mL bovine serum albumin (BSA) and 5 μ M/mlrinone to prevent meiotic resumption. For in vitro maturation, oocytes were cultured in M2 medium. The developmental process was carried out in an incubator under mineral oil at 37 °C with 5 % O₂, 5 % CO₂, and 90 % N₂. In the experimental groups, specific concentrations of FL118 were added to the culture medium for 12 h, after which oocyte maturation was further observed.

2.3. Antibodies

The following antibodies were used in this study: DDX5 (Cat#: EPR7239, dilution 1:1000; Abcam), Radixin (Cat#:13790-1-AP, dilution 1:1000; Proteintech), a mouse monoclonal antibody conjugated with FITC against α -tubulin (Cat#: F2168, dilution 1:500; Sigma), a mouse monoclonal antibody against β -actin (Cat#: AF0003, dilution 1:1000; Beyotime) and rhodamine-phalloidin (Cat#:YP0063-50T, dilution

1:1000; US EVERBRIGHT® INC). All fluorescent secondary antibodies were from Thermo Fisher.

2.4. Immunostaining

Mouse oocytes were fixed in 4 % paraformaldehyde (PFA) for 30 min and then blocked at room temperature for 1 h in phosphate-buffered saline (PBS) containing 5 % BSA and 0.5 % Triton X-100. Primary antibodies were incubated overnight at 4 °C. After three washes, secondary antibodies were applied to the oocytes for 1 h. Chromatin was stained with DAPI for 10 min. Finally, oocytes were mounted onto glass slides and examined using a Leica TCS SP8 laser scanning confocal microscope.

2.5. Western blotting

A total of 50 mouse oocytes were lysed in sample buffer and boiled at 100 °C for 5 min for Western blot analysis. The denatured proteins were then separated using 10 % sodium dodecyl sulfate-polyacrylamide gel electrophoresis (SDS-PAGE) and transferred onto a polyvinylidene difluoride (PVDF) membrane. After blocking with PBST (phosphate-buffered saline containing 5 % skim milk and 0.1 % Tween-20) at room temperature for 1 h, the membrane was incubated overnight at 4 °C with rabbit anti-DDX5 antibody (1:1000; Abcam) and mouse anti- β -actin antibody (1:1000; Beyotime). Following three washes with PBST, the membrane was incubated with horseradish peroxidase (HRP)-conjugated secondary antibodies in blocking buffer for 1 h. After three additional washes with PBST, protein bands were visualized using the ECL Plus Western Blot Detection System (GE Healthcare).

2.6. RNA-seq and gene enrichment analysis

To maintain germinal vesicle (GV) arrest, GV-stage oocytes were cultured in medium supplemented with 5 μ M milrinone and 10 μ M FL118 for 16 h. Three sample groups were collected, each consisting of five control oocytes and five DDX5i metaphase II (MII) oocytes. The RNA sequencing (RNA-seq) procedure included sample quality assessment, library construction, quality control, and high-throughput sequencing. RNA-seq was conducted using the Illumina NovaSeq 6000 platform to sequence all mRNA transcripts expressed in specific eukaryotic tissues or cells at a given time. Library construction was performed using the Illumina TruSeq™ RNA Sample Prep Kit. The RNA-seq analysis workflow included quality control, alignment, quantification, differential expression analysis, and functional enrichment analysis.

2.7. Immunoprecipitation combined with mass spectrometry identification

Ovaries were collected from 3-week-old female ICR mice at 44–46 h after PMSG injection. Four ovaries were pooled as one group, and immunoprecipitation (IP) of DDX5 was performed on the samples after lysis. Briefly, DDX5 antibody was incubated with ovarian lysate, followed by the addition of magnetic beads to capture the antibody-antigen complex. Co-precipitated proteins were analyzed by mass spectrometry (Thermo Scientific™ Q Exactive™ HFX). The mass spectrometry data were analyzed using Proteome Discoverer 2.4.

2.8. Data analysis

Statistical differences between two groups were assessed using Student's t-test. For multiple comparisons involving more than two groups, one-way analysis of variance (ANOVA) was first performed, followed by Tukey's honestly significant difference (HSD) test using R 4.2. P-value ≤ 0.05 was considered statistically significant. Unless otherwise specified, data are presented as the mean \pm SEM (standard error of the mean) from at least three independent experiments.

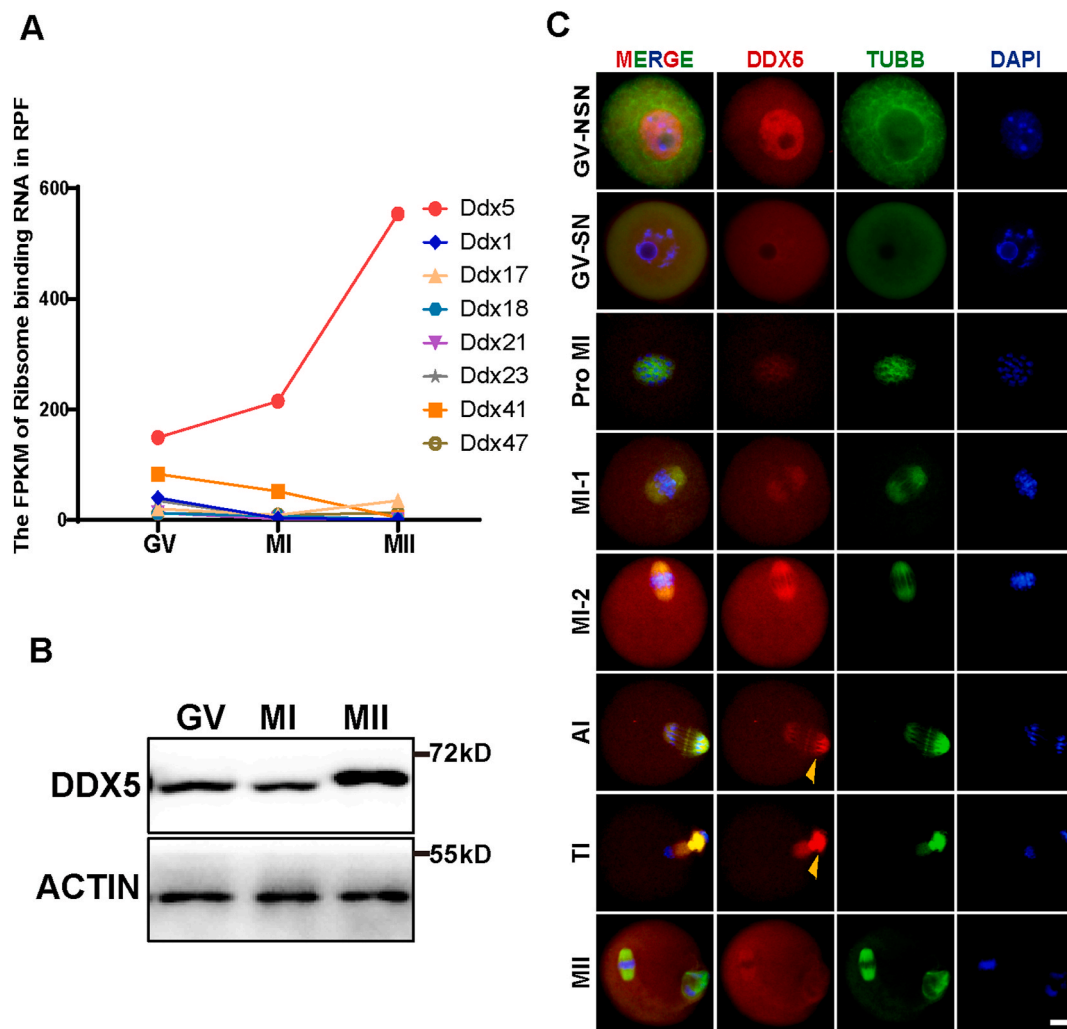


Fig. 1. Expression and Localization of DDX5 During Oocyte Meiotic Maturation

(A) FPKM values of selected DDX family proteins in oocytes at different stages (GV, MI, MII). (B) Western blot showing the dynamic expression of DDX5 protein during mouse oocyte meiotic maturation. GV, germinal vesicle; MI, metaphase I; MII, metaphase II. Each lane represents 50 oocytes. (C) Immunofluorescence images showing the specific localization of DDX5 at various stages of oocyte meiotic maturation. GV-NSN, germinal vesicle oocytes with non-surrounded nucleolus (NSN) configuration; GV-SN, germinal vesicle oocytes with surrounded nucleolus (SN) configuration; Pro-MI, prophase I; MI, metaphase I; AI, anaphase I; TI, telophase I; MII, metaphase II. Scale bar: 20 μ m.

3. Results

3.1. Expression and Localization of DDX5 during oocyte meiotic maturation

We first reanalyzed the dynamic changes of major protein members of the RNA helicase DEAD-box family during oocyte meiotic maturation. Ribosome-bound mRNA sequencing data revealed that *Ddx5* mRNA levels increased progressively during oocyte maturation, specifically at the germinal vesicle (GV), metaphase I (MI), and metaphase II (MII) stages. Notably, *Ddx5* expression at the MII stage was threefold higher than at the GV stage (Fig. 1A). Subsequently, we confirmed the expression of DDX5 at the GV, MI, and MII stages using Western blot analysis (Fig. 1B). The high expression of DDX5 during oocyte maturation suggests its potential critical role in this process.

To investigate the function of DDX5 during oocyte meiotic maturation, we performed immunofluorescence staining to determine its dynamic localization. In GV-NSN (non-surrounded nucleolus) stage oocytes, DDX5 was localized within the nucleus. However, as the nucleus condensed into the SN (surrounded nucleolus) stage, DDX5 was no longer detected in the nucleus. Notably, after germinal vesicle

breakdown (GVBD) and the resumption of meiosis, DDX5 exhibited significant colocalization with the spindle, as marked by TUBULIN, during the metaphase, anaphase, and telophase stages of meiosis (Fig. 1C). These findings suggest that DDX5 may play a role in regulating the progression of oocyte meiosis.

3.2. Inhibition of DDX5 disrupts oocyte meiotic maturation

To explore the effects of DDX5 loss of function on oocyte meiotic maturation, we inhibited DDX5 activity at the GV stage using FL118 (10,11-(Methylenedioxy)-20(S)-camptothecin), a specific inhibitor of DDX5. FL118 acts as a "molecular glue degrader," directly binding to and functionally dephosphorylating and degrading DDX5 via the proteasomal degradation pathway without affecting DDX5 mRNA levels (Fig. 2A and B) [15]. Western blot analysis of GV-stage oocytes confirmed that FL118 significantly reduced DDX5 protein levels (Fig. 2C). Following DDX5 inhibition, no significant difference in GVBD rates was observed between the control and DDX5i (DDX5-inhibited) groups 120 min after release from milrinone (Fig. 2D). However, the first polar body (Pb1) extrusion rate, which marks the completion of the first meiotic division and entry into the second meiotic arrest at MII, was reduced in the

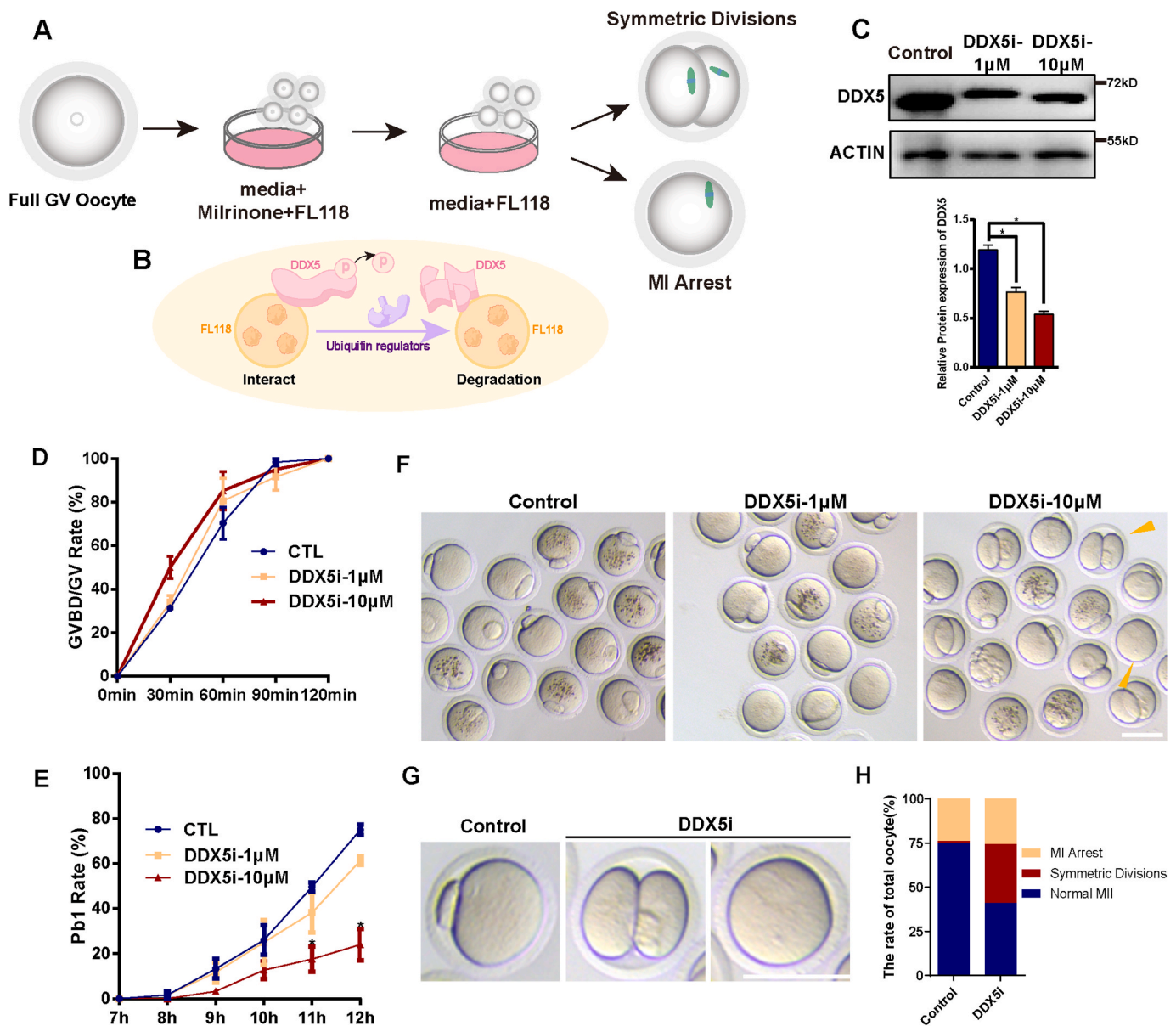


Fig. 2. Inhibition of DDX5 Function Affects Oocyte Meiotic Maturation

(A) Schematic diagram illustrating the impact of DDX5 loss-of-function on oocyte meiotic maturation. The DDX5 inhibitor FL118 was added to milrinone-containing medium, and after 16 h of inhibition, oocytes were cultured in vitro in medium containing FL118. (B) FL118 binds to DDX5, leading to its dephosphorylation and subsequent degradation via ubiquitination. (C) Western blot showing the efficiency of DDX5 protein inhibition and dephosphorylation-mediated degradation in oocytes treated with varying concentrations of FL118. Quantitative analysis of protein levels in DDX5i oocytes from three independent experiments. * $p < 0.05$. Each lane represents 50 oocytes. (D) Germinal vesicle breakdown (GVBD) rates recorded every 30 min * $p < 0.05$. (E) Hourly rates of first polar body (Pb1) extrusion in control and DDX5i oocytes. Data are presented as mean \pm SEM. * $p < 0.05$. ≥ 180 oocytes were analyzed. (F) Representative images of control and DDX5i oocytes after 13 h of in vitro maturation. Arrows indicate oocytes with developmental abnormalities. Scale bar: 100 μ m. (G) Enlarged images of abnormal oocytes from (F). Scale bar: 100 μ m. (H) Proportions of three oocyte states in control and DDX5i groups after 13 h of in vitro maturation. Cumulative analysis of >180 oocytes.

DDX5i group. Specifically, Pb1 extrusion rates decreased at 1 μ M FL118 and dropped significantly to 20 % at 10 μ M FL118 (Fig. 2E). Imaging revealed that abnormal oocyte morphology in the DDX5i group was primarily characterized by failure to extrude Pb1 and the presence of larger polar bodies, with some oocytes exhibiting near-equal cytoplasmic division (Fig. 2F-2H). These results demonstrate that inhibition of DDX5 significantly impairs oocyte meiotic maturation.

3.3. Loss of DDX5 function causes abnormal cytoplasmic division in oocytes

To further investigate the impact of DDX5 function loss on meiotic

division in oocytes, we used Tubulin to label microtubules and F-actin to label microfilaments. Immunofluorescence experiments on oocytes matured in vitro for 12 h revealed that the proportion of oocytes with significant polar body morphology was 1 % in the control group compared to 35 % in the DDX5i group. The proportion of oocytes blocked in metaphase I (MI) was 10 % in the control group and 40 % in the DDX5i group. Specifically, in the DDX5i group, oocytes blocked in MI exhibited spindle migration towards the cortical region, with the spindle being obstructed in the actin cap region, thus preventing further division (Figure 3A-3C). Additionally, real-time imaging using a time-lapse system showed that DDX5i-1 oocytes displayed abnormal cytoplasmic division at 10 h of in vitro maturation (IVM). DDX5i-2 oocytes at

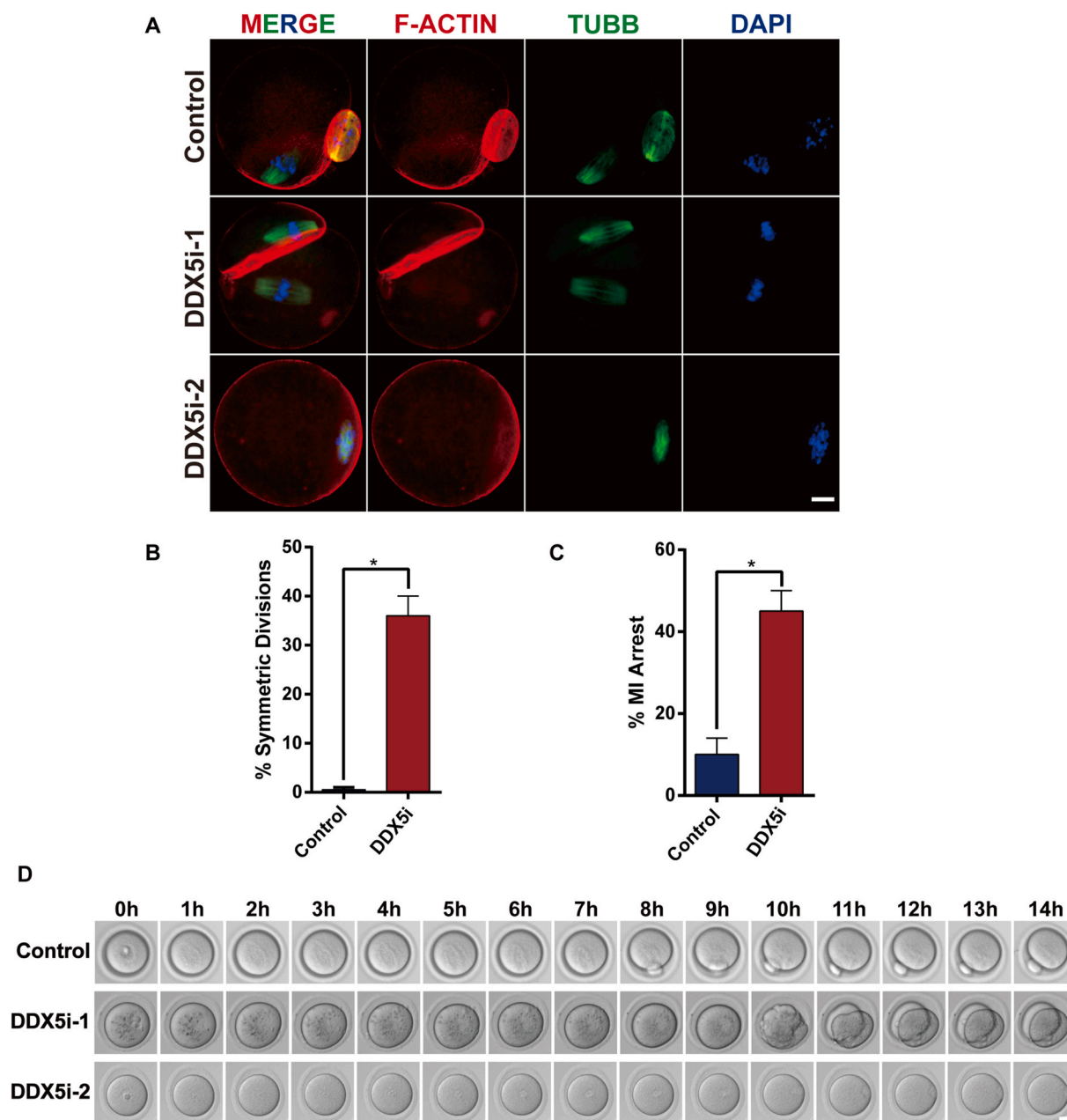


Fig. 3. Loss of DDX5 Function Leads to Cytokinesis Abnormalities in Oocytes

(A) Representative immunofluorescence images of DDX5i and control oocytes. DNA is shown in blue, F-actin in red, and α -tubulin in green. Scale bar: 20 μ m. (B) Proportion of oocytes with symmetrical cytoplasmic distribution in DDX5i and control groups. (C) Proportion of oocytes arrested at the MI stage in DDX5i and control groups. The experiment was repeated three times, with >30 oocytes per replicate and a total of >150 oocytes analyzed. (D) Schematic diagram of the developmental progression of DDX5i and control oocytes in a time-lapse imaging system. Arrows indicate spindle positions due to inconsistent refractive indices. Scale bar: 50 μ m. (For interpretation of the references to colour in this figure legend, the reader is referred to the Web version of this article.)

14 h of IVM exhibited spindle localization (a spindle-shaped structure with a relatively high refractive index) in the cortical region (Fig. 3D). These results indicate that the inhibition of DDX5 function leads to abnormal cytoplasmic division in oocytes.

3.4. Loss of DDX5 function affects the stability of mRNA in oocytes

Oocytes store a large amount of mRNA to support meiotic division and early embryo development. DDX5 is an RNA-binding protein containing a DEAD-Box/Helicase ATP binding domain capable of binding RNA [16]. To investigate the impact of DDX5 function loss on mRNA stability in oocytes, we conducted RNA-seq analysis. The results revealed significant transcriptional changes in oocytes from the DDX5i

group compared to the control group, with 249 genes upregulated and 452 genes downregulated (p -value < 0.05 & |FoldChange| > 2) (Fig. 4A and B). Pathway enrichment analysis of downregulated differentially expressed genes showed enrichment in pathways such as "microtubule-based movement", "response to oxidative stress", "female gamete generation" and "oogenesis" (Fig. 4C). Gene Set Enrichment Analysis (GSEA) further highlighted the suppression of key signaling pathways involved in oocyte development (Fig. 4D). Notably, genes related to "microtubule-based movement" signaling pathway, such as "Kif22", "Dnah7a", "Ropn1l" were significantly downregulated. Moreover, important genes associated with "alpha-tubulin binding", including "Ppargc1a", "Efhc1", "Washc1", and those related to "oocyte maturation", such as "Edn1", "Zar1l", "Washc1", "Dmc1", exhibited drastic downregulation (Fig. 4E-4G).

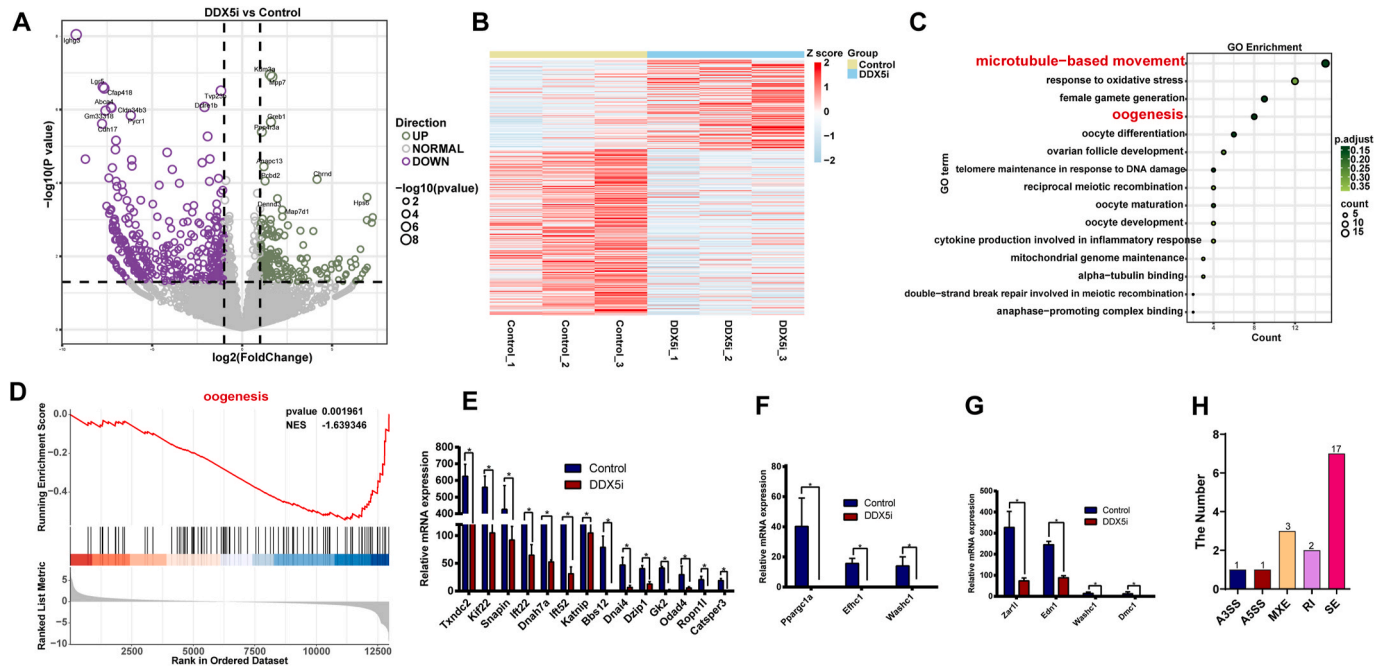


Fig. 4. Inhibition of DDX5 Function Disrupts mRNA Homeostasis in Oocytes

(A) Volcano plot showing significant transcriptomic changes in DDX5i oocytes. Vertical dashed lines indicate $p = 0.01$, and horizontal dashed lines represent a fold change of 2. (B) Heatmap displaying differential transcript expression between CTL and DDX5i oocytes. Rows represent genes, and columns represent samples. Color coding indicates gene expression levels, with red for high expression and blue for low expression. (C) GO enrichment analysis of differentially expressed genes in DDX5i oocytes, highlighting major signaling pathways. (D) GSEA analysis showing suppression of the "oogenesis" signaling pathway in DDX5i oocytes. (E, F, G) Bar graphs showing changes in FPKM values of representative genes associated with "microtubule-based movement," "alpha-tubulin binding," and "oocyte maturation." * $p < 0.05$. (H) Statistics of alternative splicing events in DDX5i oocytes compared to controls. A3SS (Alternative 3' splice site); A5SS (Alternative 5' splice site); MXE (Mutually exclusive exon usage); RI (Retained Intron); SE (Skipped Exon). (For interpretation of the references to colour in this figure legend, the reader is referred to the Web version of this article.)

Literature reports indicate that DDX5 possesses mRNA splicing functionality [17]. In the DDX5i group of oocytes, alternative splicing events were also observed to undergo changes (Fig. 4H). These findings suggest that the loss of DDX5 protein function severely disrupts mRNA stability in oocytes and affects the signaling pathways associated with spindle migration.

3.5. Loss of DDX5 function affects the expression and function of microfilament cytoskeleton proteins

To further investigate the molecular mechanisms by which DDX5 regulates meiotic division maturation in oocytes, we conducted IP-MS (immunoprecipitation combined with mass spectrometry) experiments on ovarian tissue to identify proteins interacting with DDX5. The IP-MS experiment identified 669 proteins interacting with DDX5 (with at least 3 peptides). To determine whether DDX5 protein regulates oocyte maturation by directly affecting mRNA stability or through protein interactions, we intersected genes showing differential changes in RNA-seq data with proteins interacting with DDX5, revealing only 11 genes in common. These intersecting genes accounted for only 1.6 % of the proteins interacting with DDX5 (Fig. 5A and B). Therefore, our focus shifted to investigating the molecular mechanisms of DDX5 interacting proteins.

Gene ontology enrichment analysis of DDX5 interacting proteins indicated enrichment primarily in "Actin cytoskeleton organization" and "Motor proteins." This suggests that DDX5 may influence the dynamic changes of microfilament cytoskeleton proteins (Fig. 5C). Abnormal cytoplasmic division in oocytes has been associated with dysfunctional microfilament proteins [18]. Radixin were identified as major interacting proteins in the DDX5 IP experiment (Fig. 5D). Radixin is a cytoskeletal protein that plays a potential role in linking actin to the oocyte membrane [7,19]. Western blot experiments on oocytes from the DDX5i

group revealed a significant decrease in the expression of radixin protein (Fig. 5E and F). These results indicate that DDX5 can influence the stability of microfilament cytoskeleton proteins, thereby regulating cytoplasmic division in oocytes.

4. Discussion

This study elucidates the critical role of DDX5 in regulating meiosis in mouse oocytes. Among the various members of the DEAD-box helicase family, DDX5 exhibits a unique expression pattern, with its protein levels progressively increasing during the GV, MI, and MII stages, significantly surpassing those of other family members. We further confirmed that DDX5 co-localizes with the spindle apparatus during meiotic maturation. Upon inhibition of DDX5 function, a notable downregulation of transcripts associated with the "microtubule-based movement" pathway was observed. Although abnormal cytokinesis is the primary phenotype observed in the DDX5i group, we also found that DDX5 inhibition leads to abnormal spindle assembly. This is primarily characterized by reduced microtubule stability. Since chromosomes are pulled by the spindle, abnormalities in spindle assembly result in an increased proportion of chromosome misalignment (Fig. S1). Additionally, the primary phenotypic consequence of DDX5 inhibition was the formation of an enlarged first polar body, indicating that DDX5 regulates the asymmetric cytoplasmic division of oocytes in a distinctive manner.

In somatic cells, DEAD-box helicase 5 (DDX5), an ATP-dependent RNA helicase, has been implicated in various aspects of RNA processing, including splicing, mRNA export, transcript stability, and microRNA processing [17,20,21]. In mouse oocytes, our study revealed significant alterations in the transcriptome of the DDX5i group, with the number of downregulated genes being twice that of upregulated transcripts. Fully mature oocytes are known to cease transcription, and these downregulated transcripts are degraded through post-transcriptional

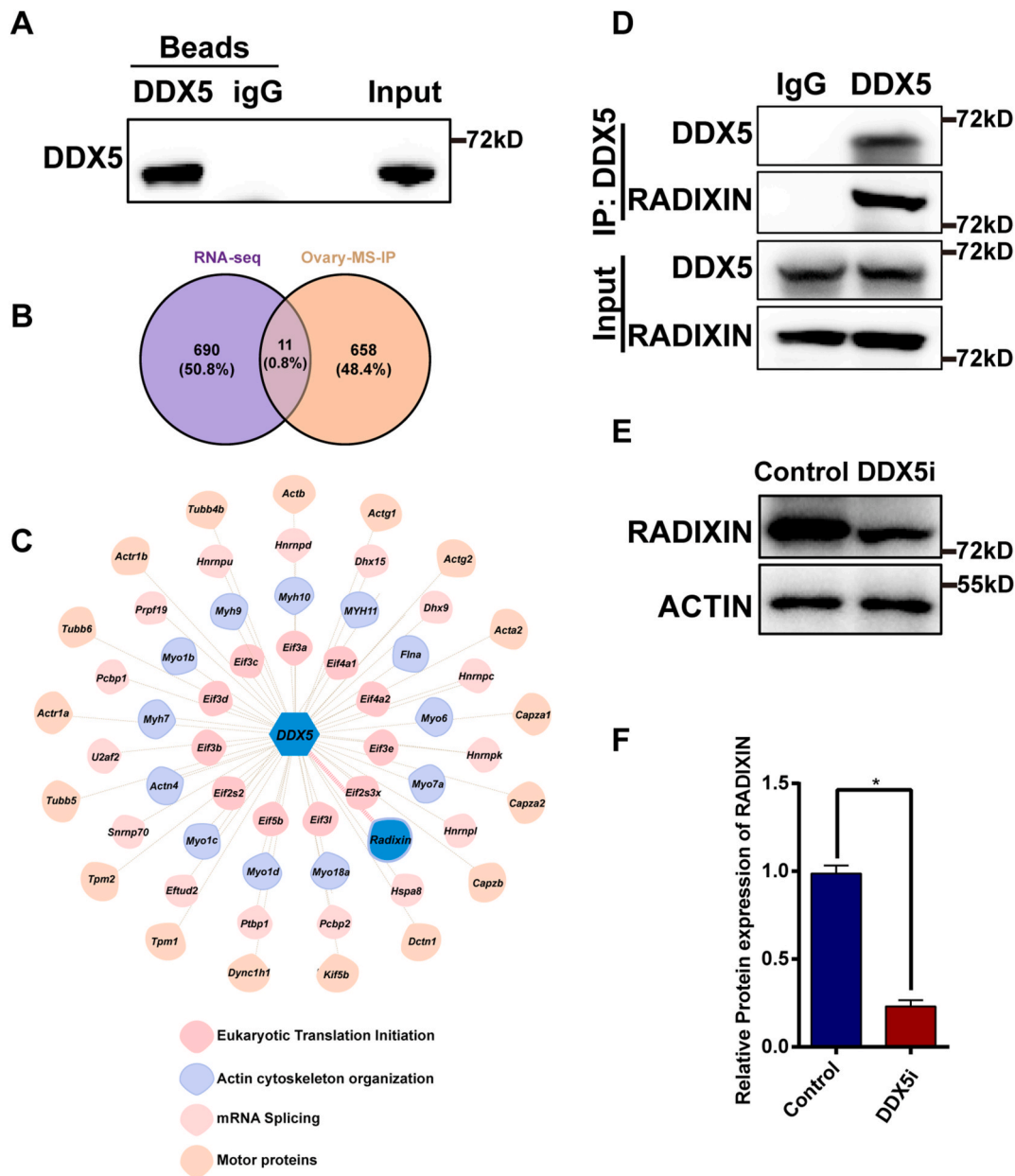


Fig. 5. Loss of DDX5 Function Affects the Expression and Function of Microfilament-Associated Proteins

(A) Endogenous IP of DDX5 antibody in ovarian tissue. (B) Venn diagram showing overlap between differentially expressed genes in DDX5i oocytes and DDX5-interacting proteins in the ovary. (C) Characteristics of DDX5-binding proteins identified by immunoprecipitation-mass spectrometry (IP-MS). (D) Endogenous IP of DDX5 antibody in ovarian tissue, demonstrating interaction with RADIXIN protein. (E, F) RADIXIN protein expression in GV-stage oocytes after 24 h of DDX5 inhibition. Quantitative analysis of RADIXIN protein levels in DDX5i oocytes from three independent experiments. Data are presented as mean \pm SEM. * $p < 0.05$. Each lane represents 50 oocytes.

regulation. Similarly, upon DDX5 inhibition, alternative splicing events of mRNAs within oocytes also exhibited differential changes. Despite the substantial changes in transcripts observed in the DDX5i group, the signaling pathways associated with the differentially expressed genes did not directly correlate with the phenotype of abnormal cytoplasmic division. This suggests that DDX5 may not directly regulate oocyte cytoplasmic division by influencing transcript homeostasis. The findings regarding DDX5 in oocytes are consistent with its known functions in somatic cells.

According to the "central dogma", proteins serve as the primary molecular machinery enabling cellular functions. To elucidate the molecular mechanisms by which DDX5 directly regulates oocyte meiosis, we conducted IP-MS to identify DDX5-interacting proteins. Our results revealed that DDX5-associated proteins are enriched in pathways

related to "Actin cytoskeleton organization" and "Motor proteins." These proteins are directly involved in regulating the assembly of actin microfilaments, thereby contributing to the formation of the actin cap and playing a critical role in inducing asymmetric division in oocytes [4–6]. Among these, we confirmed interactions between DDX5 and actin-binding protein radixin. Upon DDX5 inhibition, radixin levels in oocytes decreased by nearly 70 %.

Radixin is known to directly pull actin toward the cortical region while influencing the formation of the microfilament network [7,8]. Additionally, the typical microtubule spindle is accompanied and surrounded by actin microfilaments, referred to as spindle-actin [22]. During spindle migration, the spindle can be displaced from the oocyte center by cytoplasmic actin forces, while actin microfilaments extending from the spindle pole near the cortex anchor and stabilize the spindle at

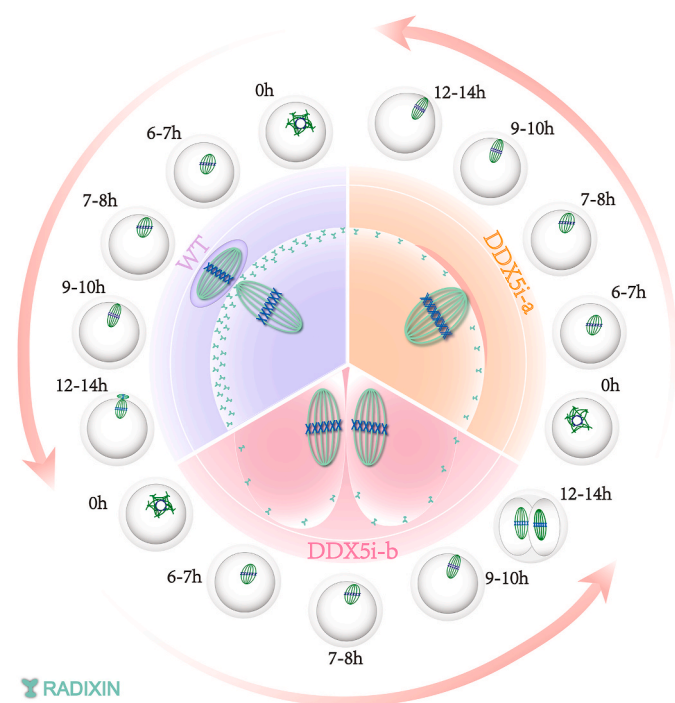


Fig. 6. Schematic Model of DDX5 Regulation in Oocyte Meiotic Maturation

DDX5 influences the dynamic migration of microfilaments and microtubules in oocytes by regulating the expression of the microfilament-binding protein RADIXIN, thereby modulating the extrusion of the first polar body. Inhibition of DDX5 leads to downregulation of RADIXIN, resulting in impaired first polar body extrusion or cytokinesis abnormalities.

the cortex, thereby promoting asymmetric oocyte division [23,24]. The decrease in the PBE (polar body extrusion) rate induced by DDX5 inhibition may result from the reduction of the actin assembly protein Radixin, which subsequently disrupts the ability of microfilaments to exert pulling forces on the spindle. We propose that DDX5 regulates asymmetric division in mouse oocytes by modulating the protein stability of the actin-binding protein radixin (Fig. 6).

5. Conclusion

Overall, our study revealed that the DEAD-box RNA deconjugating enzyme DDX5 was abundantly expressed during mouse oocyte maturation and co-localized with the spindle. Loss of DDX5 function induced aberrant cytoskeletal assembly, which, in turn, led to the failure of asymmetric division of oocytes. The cause of the abnormal cytoplasmic division of oocytes was associated with a significant decrease in the expression of radixin, an important microfilament skeleton protein. Based on the important role of DDX5 in oocytes, its in-depth mechanism still deserves further exploration.

CRedit authorship contribution statement

Lina Yu: Writing – original draft, Resources, Methodology, Investigation, Data curation. **Ruixin Shi:** Writing – original draft, Resources, Methodology, Investigation, Data curation. **Yan Mao:** Methodology, Investigation, Data curation. **Aolei Guo:** Data curation. **Lihua Zhu:** Writing – review & editing, Validation. **Guangyi Cao:** Writing – review & editing, Funding acquisition.

Data availability statement

Publicly available datasets used in this work (Fig. 1A) were from

NCBI GEO accession number GSE165782 [25]. The data that support the findings of this study are available from the corresponding author upon reasonable request.

Institutional review board statement

The animal study was reviewed and approved by the Institutional Animal Care and Use Committee of Nanjing Drum Tower Hospital (SYXK 2021–0509).

Funding

This work was supported by the National Natural Science Foundation of China (82471691), the State Key Laboratory of Reproductive Medicine and Offspring Health (SKLRM-2022D2) and Clinical Trials from Nanjing Drum Tower Hospital, Affiliated Hospital of Medical School, Nanjing University(2023-LCYJ-PY-35).

Declaration of competing interest

The authors declare that they have no known competing financial interests or personal relationships that could have appeared to influence the work reported in this paper.

Appendix A. Supplementary data

Supplementary data to this article can be found online at <https://doi.org/10.1016/j.theriogenology.2025.117401>.

References

- [1] Coticchio G, et al. Oocyte maturation: gamete-somatic cells interactions, meiotic resumption, cytoskeletal dynamics and cytoplasmic reorganization. *Hum Reprod Update* 2015;21(4):427–54.
- [2] Brunet S, Verlhac MH. Positioning to get out of meiosis: the asymmetry of division. *Hum Reprod Update* 2011;17(1):68–75.
- [3] Sun SC, Kim NH. Molecular mechanisms of asymmetric division in oocytes. *Microsc Microanal* 2013;19(4):883–97.
- [4] Mogessie B, Scheffler K, Schuh M. Assembly and positioning of the oocyte meiotic spindle. *Annu Rev Cell Dev Biol* 2018;34:381–403.
- [5] Uraji J, Scheffler K, Schuh M. Functions of actin in mouse oocytes at a glance. *J Cell Sci* 2018;131(22).
- [6] Jo YJ, et al. Actin-capping proteins play essential roles in the asymmetric division of maturing mouse oocytes. *J Cell Sci* 2015;128(1):160–70.
- [7] Larson SM, et al. Cortical mechanics and meiosis II completion in mammalian oocytes are mediated by myosin-II and Ezrin-Radixin-Moesin (ERM) proteins. *Mol Biol Cell* 2010;21(18):3182–92.
- [8] Yang Y, Xu B, Lu W. Phosphorylated ERM regulates meiotic maturation in mouse oocytes. *Biochem Biophys Res Commun* 2024;734:150602.
- [9] Li F, et al. Role of the DEAD-box RNA helicase DDX5 (p68) in cancer DNA repair, immune suppression, cancer metabolic control, virus infection promotion, and human microbiome (microbiota) negative influence. *J Exp Clin Cancer Res* 2023; 42(1):213.
- [10] Xing Z, Ma WK, Tran EJ. The DDX5/Dbp2 subfamily of DEAD-box RNA helicases. *Wiley Interdiscip Rev RNA* 2019;10(2):e1519.
- [11] Legrand JMD, et al. DDX5 plays essential transcriptional and post-transcriptional roles in the maintenance and function of spermatogonia. *Nat Commun* 2019;10(1): 2278.
- [12] Sone R, et al. Critical roles of the ddx5 gene in zebrafish sex differentiation and oocyte maturation. *Sci Rep* 2020;10(1):14157.
- [13] Lee H, et al. RNA helicase DEAD-box-5 is involved in R-loop dynamics of preimplantation embryos. *Anim Biosci* 2024;37(6):1021–30.
- [14] Zhu W, et al. Comparative proteomic landscapes elucidate human preimplantation development and failure. *Cell* 2025;188(3):814–31. e21.
- [15] Ling X, et al. FL118, acting as a ‘molecular glue degrader’, binds to dephosphorylates and degrades the oncoprotein DDX5 (p68) to control c-Myc, survivin and mutant Kras against colorectal and pancreatic cancer with high efficacy. *Clin Transl Med* 2022;12(5):e881.
- [16] Linder P, Jankowsky E. From unwinding to clamping - the DEAD box RNA helicase family. *Nat Rev Mol Cell Biol* 2011;12(8):505–16.
- [17] Dardenne E, et al. RNA helicases DDX5 and DDX17 dynamically orchestrate transcription, miRNA, and splicing programs in cell differentiation. *Cell Rep* 2014; 7(6):1900–13.
- [18] Almonacid M, Terret ME, Verlhac MH. Actin-based spindle positioning: new insights from female gametes. *J Cell Sci* 2014;127(Pt 3):477–83.
- [19] Miller KG. A role for moesin in polarity. *Trends Cell Biol* 2003;13(4):165–8.

- [20] Lin C, et al. ATPase/helicase activities of p68 RNA helicase are required for pre-mRNA splicing but not for assembly of the spliceosome. *Mol Cell Biol* 2005;25(17):7484–93.
- [21] Li H, et al. RNA helicase DDX5 inhibits reprogramming to pluripotency by miRNA-based repression of RYBP and its PRC1-dependent and -independent functions. *Cell Stem Cell* 2017;20(4):571.
- [22] Azoury J, et al. Spindle positioning in mouse oocytes relies on a dynamic meshwork of actin filaments. *Curr Biol* 2008;18(19):1514–9.
- [23] Chaigne A, et al. A narrow window of cortical tension guides asymmetric spindle positioning in the mouse oocyte. *Nat Commun* 2015;6:6027.
- [24] Yi K, et al. Sequential actin-based pushing forces drive meiosis I chromosome migration and symmetry breaking in oocytes. *J Cell Biol* 2013;200(5):567–76.
- [25] Xiong Z, et al. Ultrasensitive Ribo-seq reveals translational landscapes during mammalian oocyte-to-embryo transition and pre-implantation development. *Nat Cell Biol* 2022;24(6):968–80.